

Neutron- and muon-induced background in underground physics experiments

V. A. Kudryavtsev¹, L. Pandola², and V. Tomasello¹

¹ Department of Physics and Astronomy, University of Sheffield, Sheffield, United Kingdom

² INFN, Laboratori Nazionali del Gran Sasso, Assergi, Italy

Received: date / Revised version: date

Abstract. Background induced by neutrons in deep underground laboratories is a critical issue for all experiments looking for rare events, such as dark matter interactions or neutrinoless $\beta\beta$ decay. Neutrons can be produced either by natural radioactivity, via spontaneous fission or (α, n) reactions, or by interactions initiated by high-energy cosmic rays. In all underground experiments, Monte Carlo simulations of neutron background play a crucial role for the evaluation of the total background rate and for the optimization of rejection strategies. The Monte Carlo methods that are commonly employed to evaluate neutron-induced background and to optimize the experimental setup, are reviewed and discussed. Focus is given to the issue of reliability of Monte Carlo background estimates.

PACS. 98.70.Sa Cosmic rays – 98.70.Vc Background radiations – 95.35.+d Dark matter – 23.40.-s Double beta decay

1 Introduction

The key issue for all experiments looking for rare events, such as dark matter interactions, neutrinoless $\beta\beta$ decay, low-energy neutrinos, etc., is the suppression and rejection of the background due to cosmic rays and natural radioactivity. The former is reduced by operating the experiments in deep underground laboratories: the rock shielding, a few km of water equivalent (w. e.), allows the reduction of the flux of cosmic ray muons by a factor of $10^5 - 10^7$ with respect to the surface. Background due to natural radioactivity (mainly γ -rays) can be suppressed by means of passive shielding or rejected by specific identification tools, depending on the experimental design (*e.g.* γ -recoil discrimination for dark matter experiments, single-site selection for neutrinoless $\beta\beta$ decay experiments).

Neutrons are more penetrating than γ -rays and they are a dangerous background source for most underground experiments. In dark matter experiments looking for direct interactions of WIMPs (Weakly Interacting Massive Particles), neutron background is critical because elastic interactions of fast neutrons give the very same signature as the signal, namely the WIMP elastic scattering off a nucleus. Similarly, γ -rays emitted in neutron inelastic scattering ($n, n'\gamma$) or capture (n, γ) (prompt or delayed) may mimic the signature of the neutrinoless $\beta\beta$ decay. Also unstable nuclei produced in neutron-nucleus interactions are potential background sources in experiments looking for neutrinoless $\beta\beta$ decay.

Hence, in order to predict and optimize the sensitivity of underground experiments, the background induced

by neutrons must be precisely characterized. Monte Carlo simulations play a crucial role in this field, because:

1. They can predict the neutron flux expected in an underground laboratory (as well as the energy spectrum) and the corresponding background rate due in a real experiment.
2. They can be used to study background suppression or rejection strategies, and to investigate requirements on the depth, the amount of active/passive shielding, the minimum veto efficiency, etc., for a given experiment.

In this paper the Monte Carlo tools and methods that can be used to quantify neutron-induced background in underground experiments are reviewed. The actual validity of the Monte Carlo based calculation, and the achievable precision are also discussed. Finally, some considerations are presented about the most effective tools to reduce and suppress neutron background for underground physics experiments. The study has been focused on the experiments that are involved in the EU ILIAS integrated activity [1], and on the four underground Laboratories in the ILIAS network, namely Gran Sasso (Italy), Modane (France), Canfranc (Spain) and Boulby (United Kingdom). The minimal depth of these underground sites is between 2.5 and 4 km w. e.

2 Natural neutron sources in underground laboratories

Neutrons in deep underground laboratories are produced in reactions initiated either by natural radioactivity or by cosmic rays.

Neutron flux due to natural radioactivity (in the rock around the laboratory and/or in the materials of the experimental setup) is produced by: (1) spontaneous fission, the most important source being ^{238}U , and (2) (α, n) interactions of α 's from natural α -emitters ($E_\alpha < 10$ MeV) with light target nuclei. For heavy nuclei the (α, n) cross section is suppressed by the Coulomb barrier. Neutrons from natural radioactivity have energy up to about 10 MeV.

Neutrons are also produced in nuclear reactions (*e.g.* muon-, photon- or hadron-induced spallation or disintegration) induced by cosmic ray muons. These reactions can be caused by the muon itself (muon-induced spallation or negative muon capture) or by secondary particles (photons and hadrons) generated in muon-induced cascades in the rock or in the materials of the experimental setup. The energy spectrum of these neutrons is substantially harder compared to neutrons from radioactivity. Neutrons can be emitted with energies up to a few GeV.

The relative importance of neutron-induced background coming from these two sources (natural radioactivity and cosmic rays) is very much dependent on the depth of the underground laboratory and on the specific experimental design, namely presence and thickness of passive shielding, muon vetoes, materials, etc. The Monte Carlo methods that are used to estimate the neutron flux in an underground laboratory and the neutron-induced background in a given detector are described in detail in sects. 3 and 4.

3 Neutrons from natural radioactivity

3.1 Ingredients for the calculation

The ‘‘ingredients’’ that are needed for the evaluation of the background induced in a given setup by neutrons from natural radioactivity are as follow:

1. The chemical composition of the source material (rock, detector component, etc.). The fractions of hydrogen and other light elements are particularly important because they affect in a substantial way the neutron production and/or propagation.
2. The contamination of the material in ^{238}U , which undergoes spontaneous fission¹, and in α -emitters from the U and Th natural chains. The issue of secular equilibrium of radioactive chains is important both for the total neutron production rate and for the neutron energy spectrum, because the (α, n) cross section is

¹ Other naturally occurring isotopes are known to decay by spontaneous fission. Nevertheless, the branching ratios are negligible with respect to ^{238}U .

strongly dependent on energy. High-energy α 's emitted by Po isotopes have in fact the highest probability to produce a neutron.

3. The nuclear parameters of interest. For spontaneous fission they are the multiplicity, the half-life and the relevant branching ratio; these data are available in nuclear databases for ^{238}U and for other isotopes that decay by spontaneous fission. For the (α, n) interactions it is necessary to know the interaction cross-section as a function of energy for all possible target isotopes that compose the material under investigation. It is also important to know the branching ratio for transitions of the target nucleus to the excited states, since such a transition reduces the energy of the emitted neutron.
4. The propagation of neutrons from the production point to the sensitive volume, possibly through the external passive shielding, and the neutron detection process. The particle that is eventually detected is not necessarily the primary neutron, but may also be a secondary produced by neutron interactions (*e.g.* a γ -ray from neutron capture or a recoiling nucleus). Propagation of neutrons through the experimental setup can be handled by Monte Carlo codes, such as GEANT4 [2, 3] and MCNPX [4]. FLUKA [5] is also suited for this task but has restrictions of not using point-wise cross-sections for neutron interactions and of not generating individual nuclear recoils, acting as an event signature in dark matter experiments.

The first three items are required to calculate the specific production rate of neutrons in the material under investigation, which is quoted in neutrons/(cm^3 s) or in neutrons/(kg s). The last item is required to estimate the actual background rate (counts/s) in the detector; in this case the detector properties (*e.g.* geometry, particle identification capabilities, etc.) have to be taken into account.

The specific neutron production rate per unit volume for a given material can be calculated using the code SOURCES developed in the Los Alamos Laboratory [6]. The software contains a database with tabulated (α, n) cross-sections for several targets in the energy range of natural α -emitters, energies of α 's for most α -emitters and the main properties (multiplicity, branching ratio, half-lives) for isotopes that undergo spontaneous fission. The original version of the SOURCES 4A code has been modified to extend the library of (α, n) cross-sections and the energy range of α 's up to 10 MeV, in order to include all α 's in the U and Th decay chains and more target isotopes [7]. Recently further improvements have been made to the code as part of the ILIAS project [8, 9]. More cross-sections have been added to the library as calculated using a dedicated code EMPIRE 2.19 [10]. The code has an advantage of being able to calculate branching ratios for transitions to excited states. As specified above, this makes the calculated neutron energy spectrum softer, because part of the energy is carried away by γ -rays.

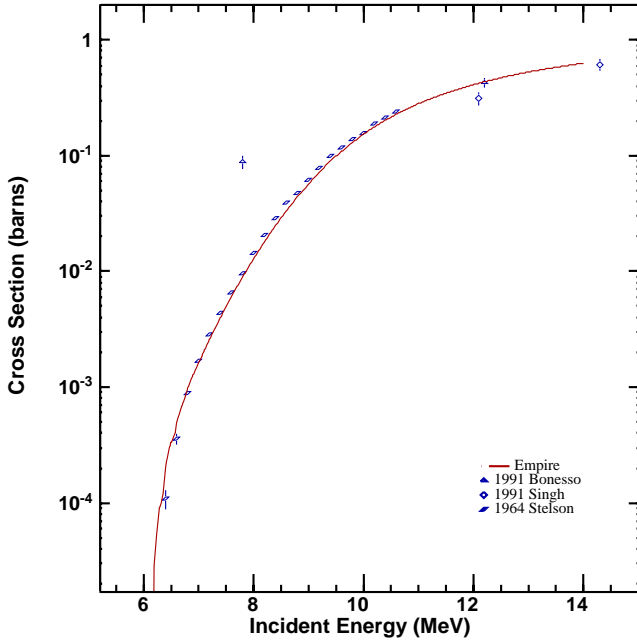


Fig. 1. Cross-section of (α, n) reactions on ^{65}Cu as a function of α energy

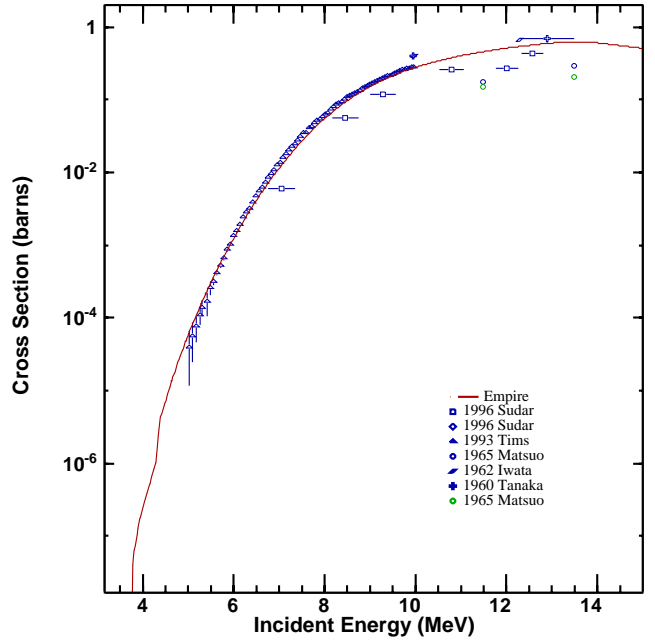


Fig. 2. Cross-section of (α, n) reactions on ^{55}Mn as a function of α energy

3.2 Validation of the Monte Carlo codes

For some target isotopes of interest experimental data on (α, n) cross-section are scarce or totally unavailable. In this case, the cross-section has to be calculated using specific models. As discussed in sect. 3.1, the cross-section database of the SOURCES 4A code has been extended using calculations from EMPIRE 2.19. To prove the robustness of the calculations of neutron production rate it is necessary to validate the EMPIRE 2.19 predictions against experimental data.

Figures 1 and 2 show the (α, n) cross-section versus energy as calculated with EMPIRE 2.19 for two isotopes, in comparison with experimental data. The agreement is better than 20% for the majority of experimental data at energies below 10 MeV that are relevant for α 's from radioactive isotopes. A large variety of tests were done to check the reliability of SOURCES 4A and an agreement with experimental data was found for both neutron yields and spectra in various materials (see, for instance, ref. [6] for discussion).

The neutron-induced background rate in a given setup depends also on the transportation of neutrons from the production point in the source material itself. The two codes that are commonly used for neutron tracking are GEANT4 and MCNPX. It has been demonstrated [8] that GEANT4 and MCNPX are in good agreement for neutron tracking in the energy range of interest and in the materials that are commonly used for neutron shielding. As shown in ref. [8], the deviation between the two codes after a mixed polyethylene/lead passive shielding is less than 50% after a six-order of magnitude suppression of neutron flux. Such a suppression is required for high-sensitivity

large-scale dark matter and $\beta\beta$ decay detectors to reduce the neutron background from rock below the experimental sensitivity level.

Further confirmation of the GEANT4 ability to model neutron propagation and detection comes from the agreement between simulations and measurements of fast (\sim MeV) neutrons from a ^{252}Cf source [11].

This demonstrates that the estimates of background due to neutrons from radioactivity in typical underground applications are reliable, with uncertainty being less than 50%.

3.3 Results

The most critical materials to be considered as neutron sources are mainly: (1) rock and concrete of the underground laboratories, that dominate the total neutron flux, and (2) materials that compose the internal detector parts (*e.g.* stainless steel, copper, PMTs etc.), that become important when the external flux is suppressed by the (radio-pure) shielding.

Figure 3 shows the neutron energy spectrum at production in rock around the Modane Underground Laboratory (LSM). It is similar to that presented in ref. [8] but has been obtained after recent improvements in the (α, n) cross-sections calculations [9]. The rock composition and U/Th concentrations were taken from ref. [8]. Separate contributions from uranium (α, n) reactions, thorium (α, n) reactions and ^{238}U spontaneous fission are shown. Spectrum of neutrons from ^{238}U spontaneous fission is described by the Watt function [12], with a peak energy of about 0.8 MeV and a mean energy of about 1.7 MeV.

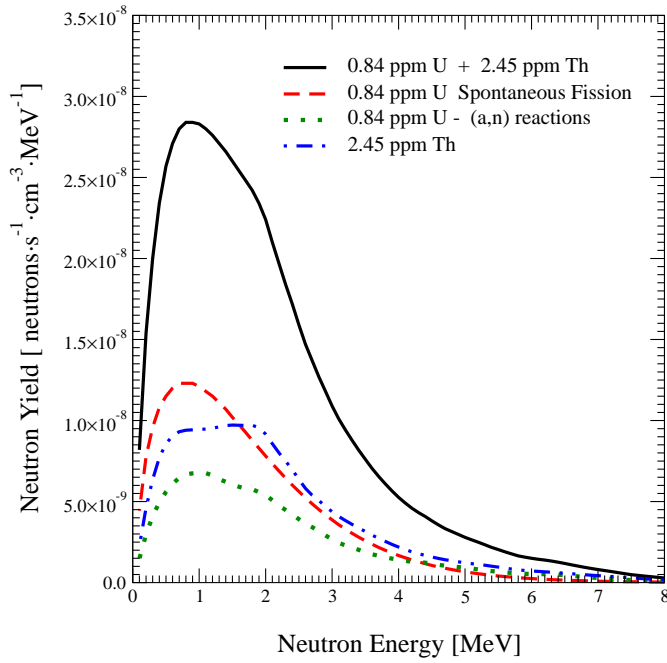


Fig. 3. Neutron energy spectra from uranium and thorium (α,n) reactions, and ^{238}U spontaneous fission in the LSM rock. The sum spectrum is shown by the solid curve.

Spectra of neutrons from (α,n) reactions are not much harder resulting in a total energy spectrum (the sum of spontaneous fission and (α,n) contributions) with a mean energy of about 1.95 MeV. In general, simulations with SOURCES taking into account the proper branching ratios for transitions to excited states, give softer neutron spectra than reported in earlier simulations and measurements (see, for instance, refs. [13,14]).

The neutron energy spectrum from U and Th in copper is shown in Figure 4. Since the energy threshold for (α,n) reactions in copper is about 7 MeV (due to high- Z and Coulomb barrier), the main contribution comes from spontaneous fission of ^{238}U . Hence, for a given U/Th concentration, copper has an advantage over other materials containing lower- Z isotopes (for instance, stainless steel).

Figure 5 shows the energy spectrum of neutrons emerging from the LSM (Modane) rock into the laboratory. Neutron transport through the rock was carried out using GEANT4 with an input spectrum from Figure 3. Concrete walls were not included in these simulations and no back-scattering of neutrons from the walls was taken into account. The latter effect increases the neutron flux above 1 MeV by about 30% [8]. Both total yield and spectral shape depend substantially on the chemical composition, in particular on the abundance of light elements and hydrogen. Hydrogen affects the thermalization and absorption of neutrons and hence suppresses the total flux. Only 1% of hydrogen reduces the neutron flux above 100 keV (1 MeV) by a factor of 4.7 (1.8) [8]. The peaks and dips on the neutron spectrum are not of statistical origin but reflect the shape of the cross-section of neutron interaction with rock. The precise knowledge of the chemical compo-

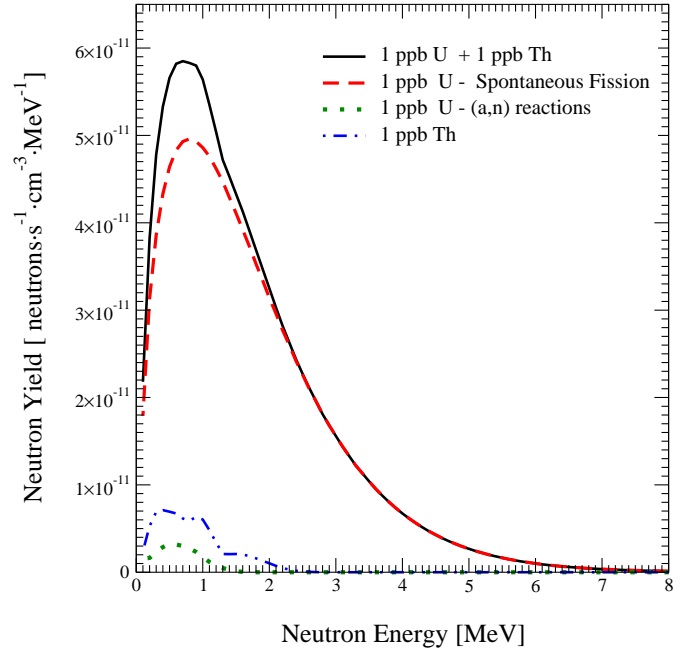


Fig. 4. Neutron energy spectra from uranium and thorium (α,n) reactions, and ^{238}U spontaneous fission in Cu. Equal concentrations of 1 ppb were assumed for uranium and thorium. The sum spectrum is shown by the solid curve.

sition of the source material and possibly of its chemical homogeneity is crucial for reliable results, since it could be a dominant source of systematic uncertainty.

Detailed comparison of the simulated neutron flux at LSM with the measurements were presented in ref. [15]. Neutron yield was calculated with the SOURCES 4A code and neutrons were propagated using MCNPX. Production of neutrons in rock and concrete was taken into account. Experimental data were taken from ref. [13], corrected using more accurate estimate of neutron detection efficiency [16]. It was found that the measured flux exceeds simulations by approximately a factor of 2 [15]. We consider this as a reasonable agreement taking into account that: (i) the conversion of the measured neutron rate in scintillator [13] into the neutron flux and spectrum requires simulations and is not free from systematic uncertainties; (ii) the rock composition and U/Th concentrations are not known with high precision since only a few samples of rock and concrete were measured; (iii) the average concentration of water in rock and concrete is difficult to measure whereas water (hydrogen) affects significantly the neutron flux in the laboratory (see the discussion above).

Similar comparison between measurements and simulations was carried out for the Boulby rock (salt) [11]. The difference of about 50% does not exceed statistical and systematic uncertainties.

The typical fast neutron flux in underground laboratories is of the order of a few 10^{-6} neutrons/($\text{cm}^2 \text{ s}$). It depends on the parameters of the laboratory rock (composition and radiopurity) and is insensitive to the depth.

In low-background experiments, neutron flux from the rock has to be suppressed by means of dedicated thick

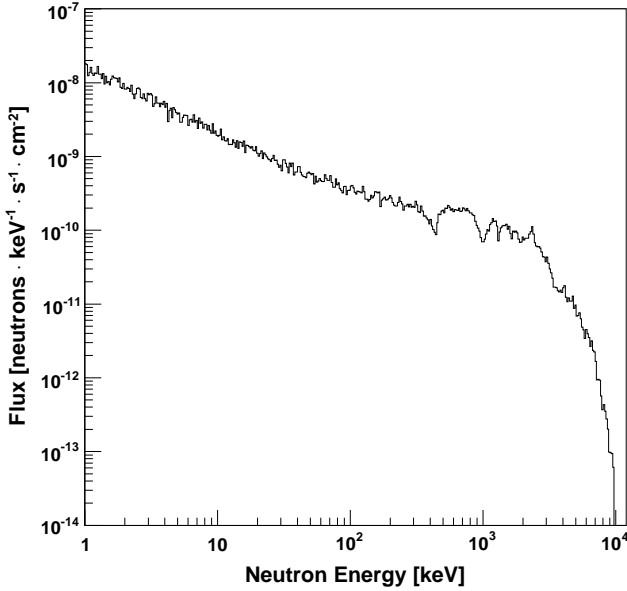


Fig. 5. Neutron energy spectrum from U and Th traces in the LSM rock. The spectrum is obtained by propagating neutrons from evenly distributed sources through rock to the laboratory walls using GEANT4.

passive shielding (polyethylene, water, etc.). A shielding thickness of about 55-60 g/cm² of polyethylene (CH₂) is sufficient to suppress the external neutron flux by six orders of magnitude, ensuring a residual background of less than 1 event/tonne/year in direct dark matter experiments [7]. Similar suppression can be achieved by using 45-50 g/cm² of CH₂ together with 20-30 cm of lead placed between the rock and CH₂. If the neutron passive shielding is in place, the dominant sources of neutron background from radioactivity are the detector components, giving 10⁻⁸ – 10⁻¹⁰ neutrons/(cm² s). For this reason, special care has to be taken of the radiopurity of the internal detector parts (including shielding) and to the optimization of passive and active shielding. Further reduction of neutron background due to radioactivity can be achieved by exploiting specific features of neutron interactions as opposed to WIMP interactions, such as, for instance, multiple nuclear recoils in the target, coincidences with active veto system, etc.

4 Neutrons from cosmic-ray muons

The other important neutron source in underground laboratories are cosmic-ray muons and muon-induced cascades or showers. Neutrons produced by cosmic rays are substantially harder (extending up to GeV energies) than those from radioactivity and are hence more difficult to suppress. Since the neutron flux is proportional to the residual muon rate at the underground site, this background can be reduced by going deeper and deeper. Nevertheless, it is important to estimate precisely the expected

neutron flux induced by cosmic rays in the existing underground sites, and to optimize the suppression and rejection tools, in order to increase as much as possible the experimental sensitivity.

4.1 Ingredients for the calculation

The calculation of the muon-induced neutron flux needs several inputs. The required “ingredients” are as follow:

1. The total muon flux at the underground site. Such a value is a specific parameter that characterizes each underground site, and is known experimentally. For instance, the residual muon flux at the Gran Sasso and Modane laboratories are about 1.1 muon/(m² hour) [17, 18, 19] and 0.23 muons/(m² hour) [20, 21], respectively². The flux obviously decreases with depth.
2. The energy spectrum and the angular distribution of muons. Energy and angle are in general correlated, depending on the particular surface profile above the underground laboratory. For laboratories located under mountains, the energy-angular distribution is determined by the structure and the orography of the region: muons come preferentially (and with softer energy spectrum) through the “valleys”, where they meet the least rock overburden. Laboratories that are excavated in mines have a more homogeneous shielding profile. Information about energy and angular distribution of muons can be obtained by experimental measurements or, in the case they are not available or not reliable, by Monte Carlo simulation. Accurate measurements of muon energy spectra underground are very difficult and one has to rely on simulations taking as an input the muon energy spectrum at surface. Several fast dedicated codes, for instance MUSIC [22], are able to track muons through large distances in different materials, and to predict reliably the energy/angular distributions, provided the rock overburden profile of the site is accurately known. Another code MUSUN [23] can be used to generate muons according to their angular and energy distribution (already obtained with MUSIC) at the underground laboratory. The average muon energy increases with the site depth: for the Gran Sasso laboratory it is about 270 GeV.
3. The code to track muons and their interactions, as well as production, propagation and possible detection of all secondaries, including neutrons. Monte Carlo codes that are commonly used for this purpose are GEANT4 and FLUKA.

The first two items simply represent an input for the Monte Carlo tracking of primary muons. The third item is the most critical step, involving the modeling of the hadronic and electromagnetic interactions in a muon-induced particle shower. Usually a large number of secondary particles are produced within the shower, neutrons being a

² Muon flux is defined here as through a sphere with unit cross-sectional area.

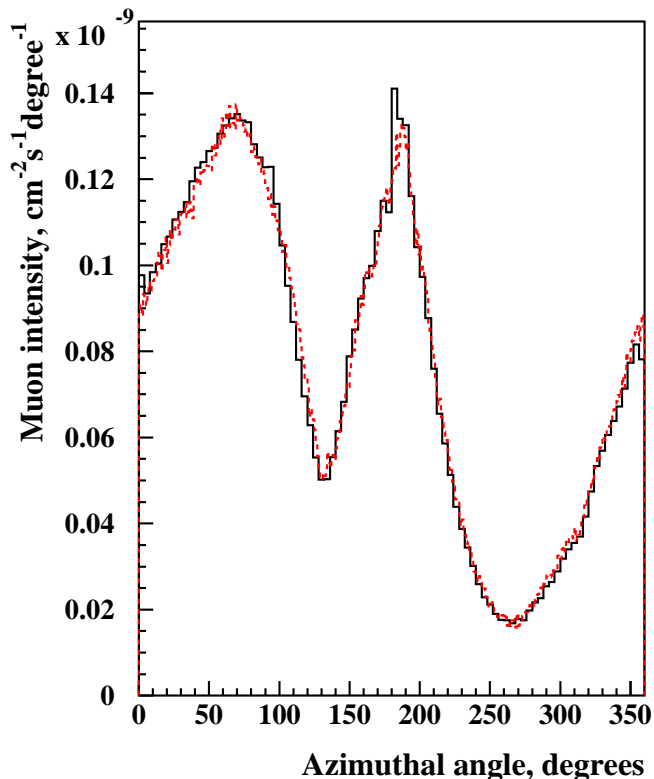


Fig. 6. Azimuthal angle distribution of single muon intensities, measured by the LVD experiment in the Hall A of the Gran Sasso Laboratory [18,19] (black histogram), superimposed on the simulation results obtained with the MUSIC/MUSUN Monte Carlo codes (red dashed histogram).

fraction of them. It is extremely important that all particles (including electrons and γ -rays) are produced in a Monte Carlo simulation and propagated through the whole setup. There is a possibility that neutrons are detected simultaneously with muons or other secondaries (interacting either in the sensitive detector or in other active volumes, such as an active veto), providing a very efficient tool for neutron background rejection.

Figure 6 shows the azimuthal angle distribution of single muon intensities as measured by the LVD experiment at Gran Sasso (solid histogram) [18,19] together with the simulated one with the MUSIC/MUSUN Monte Carlo codes. Muons were transported through the Gran Sasso rock using MUSIC, their angular distributions and energy spectra were recorded and used in MUSUN. The detector efficiencies have been taken into account when plotting the distributions. The observed agreement proves the reliability of muon simulations, as described above.

4.2 Validation of the Monte Carlo codes

Several output parameters/distributions can be derived from the Monte Carlo simulation (neutron energy and an-

gular spectra, expected background rate in a real experiment, etc.). One possible output is the integral neutron yield, which is normally quoted in neutrons per muon per g/cm^2 of crossed target material. The integral neutron yield has to be compared to experimental data for specific targets, in order to validate and cross-check the simulations.

Experimental measurements of muon-induced neutron yield are difficult because the flux is very low in deep underground laboratories. Only tonne-scale detectors are able to measure the muon-induced neutron flux with reasonable accuracy. The neutron flux can be artificially enhanced by placing a large amount of high- A material around the detector. Since the neutron yield increases with the atomic weight of the target material, high- A elements are the best targets for such measurements. Unfortunately, high- A materials cannot be used for detecting neutrons. The best neutron detectors are based on liquid scintillators that can be produced in large quantities at reasonable cost. Also dark matter experiments are very good fast neutron detectors if accompanied by a muon detector, but require a large mass of target material. Furthermore, the measurement is actually possible only at large distance from the primary muon track (otherwise the muon itself or secondary particles in muon shower are detected and single neutrons cannot be disentangled).

The total neutron yield has been reported from different measurements (see, for instance, refs. [23,24] for a compilation and discussion of experimental results). Although the authors converted their experimental results into the total yield per muon in the detecting material (*e.g.* scintillator), the measured parameter was the rate of thermal neutrons or, more precisely, the rate of γ -rays from neutron capture. As in most experiments this rate was measured using liquid scintillator, a significant part of fast neutrons was also detected through their moderation and capture in scintillator. The processes of neutron production, transport and detection are quite complicated and the precise modeling of the detector geometry, hardware and software cuts and all physical processes involved, is necessary for the accurate derivation of the neutron yield. Unfortunately this has not been achieved so far for any experiment at large depth underground. Despite the lack of accurate simulations of specific experimental setups, generic Monte Carlo results based on GEANT4 and FLUKA are found to be in a reasonable agreement (within a factor of two) [23,24,25] with the available data for low- A materials (scintillator). The overall agreement between GEANT4 and FLUKA is quite good for these materials. FLUKA predicts the dominance of hadron-induced spallation in neutron production for practically all targets, while GEANT4 favours nuclear disintegration by real photons at almost all energies (except very low energies) and all materials.

While for low- A targets the agreement between different codes and data is reasonably good (certainly within a factor of two, if we neglect possible systematic uncertainties due to the absence of precise modeling of the experimental setups), some experiments with heavy targets

showed much larger neutron yield than expected. Differential cross-section of neutron production in thin targets (graphite, copper, lead) has been measured by the NA55 experiment at CERN for 190-GeV muons [26]. The thin-target configuration does not correspond to the real situation in underground laboratories, where showers can develop through large thickness of rock but can be modeled more accurately. Experimental data have been compared to Monte Carlo simulations performed with GEANT4 and FLUKA in ref. [25]. While GEANT4 and FLUKA agree with each other within a factor of two, both codes underestimate significantly the neutron production as measured by NA55, especially for copper and lead. Yet again, a complete simulation of the NA55 detector has not been carried out by the authors of the original work and it is difficult to draw definite conclusions, because some detector-specific aspects (geometry, response) could have been neglected in ref. [25].

There are other experimental data available for neutron yield in lead, obtained in deep underground laboratories. These data are old and controversial [27, 28], but also indicate higher neutron production in lead than expected from modern Monte Carlo simulations. The issue of neutron production in lead is extremely important to underground experiments, because lead is commonly used as shielding material. More experiments are planned as part of the ILIAS activities using underground dark matter detectors or massive veto systems, accompanied by detailed Monte Carlo simulations to be used for data interpretation.

Preliminary results from the measurements of muon-induced neutrons at the Boulby Underground Laboratory have recently been reported [29]. This experiment improves on previous, even larger scale detectors, since full 3D Monte Carlo of the set-up has been carried out using GEANT4. Preliminary results suggest that GEANT4 overproduces neutrons in the materials surrounding the detector (mainly rock and lead) by about 80% compared to the measured muon-induced neutron rate. This is not consistent with the deficit of simulated neutrons discussed in ref. [23, 24, 25] (see also references therein). Detailed comparison of muon-induced neutron background as simulated with GEANT4 and FLUKA has been carried out in ref. [25]. The agreement within 20% has been found for neutron spectra in an underground laboratory located in salt rock (Boulby). Special case of muon-induced neutron background in a xenon-based dark matter experiment has also been investigated. GEANT4 and FLUKA are consistent in predicting the rate of events caused by this background to within 20% (the difference does not exceed statistical uncertainty of simulations). The observed inconsistency between measured and simulated neutron yields makes the predictions of muon-induced neutron rate in various detectors uncertain by about a factor of two.

4.3 Results

Neutron yield is dependent on the target material, ranging from a few 10^{-4} neutrons/muon/(g/cm²) for light mate-

rials (water, graphite, liquid scintillator) up to a few 10^{-3} neutrons/muon/(g/cm²) for high- A elements, such as gold and lead. Monte Carlo simulations have been used to derive a scaling law for neutron yield Y versus the atomic mass A , namely $Y \propto A^{0.8}$.

Since high- A targets, such as lead that is used for passive γ -ray shielding, have higher neutron yield, they behave like a neutron source under muon irradiation. For this reason it is necessary to include an internal low- A shielding (preferably with large amount of hydrogen, for instance, polyethylene or water) between the lead shielding and the sensitive detector, in order to reduce the muon-induced neutron background.

Neutrons produced in the rock, lead shielding or other materials of the experimental setup can be identified and tagged if the primary muon or other secondaries interact in the detector or in an active veto surrounding the detector. Indeed only neutrons that are not accompanied by other particles in the detector or in active vetoes represent a background for underground experiments. Full discussion of these issues with respect to dark matter searches can be found in ref. [25].

The typical flux of fast neutrons induced by cosmic ray muons in an underground laboratory with a rock coverage of 3000 m w. e. (as Gran Sasso or Boulby) is about 10^{-9} neutrons/(cm² s), *i.e.* three orders of magnitude smaller than the neutron flux produced by radioactivity. The flux of muon-induced neutrons is strongly dependent on the depth of the underground site, that affects the total muon flux and spectrum, as well as on the composition of the rock (density and average atomic mass $\langle A \rangle$).

Energy spectrum of muon-induced neutrons is substantially harder than that from fission or (α ,n) reactions. Figure 7 shows the neutron spectra in lead and aluminium (mean atomic weight similar to rock) from 300 GeV muons. The spectra were obtained by transporting a beam of muons (from ‘vacuum’) through a certain thickness of material and recording the secondary neutron spectrum at the boundary between the material and the vacuum beyond it. Two important conclusions can be derived from this figure. Firstly, 200 g/cm² thickness of target is too small for a neutron flux to be in equilibrium with the muon flux. Neutron flux increases as the thickness of aluminium increases to 500 g/cm². For this reason, when interpreting the data from experiments with relatively thin targets, a proper account should be taken of the development of muon-induced cascades, which is impossible to achieve without full Monte Carlo (see also ref. [25] for discussion). Secondly, the neutron energy spectrum depends strongly on the target material. All enhancement of the neutron production in lead occurs at neutron energies below 20 MeV. The flux above 20 MeV is practically material independent. Hence, high- A targets give higher neutron yield than low- A ones, but with softer energy spectrum. Similar conclusion was derived also in refs. [7, 23, 24, 25].

Figure 8 shows the neutron energy spectra produced by muons with energies 100 GeV and 300 GeV in lead

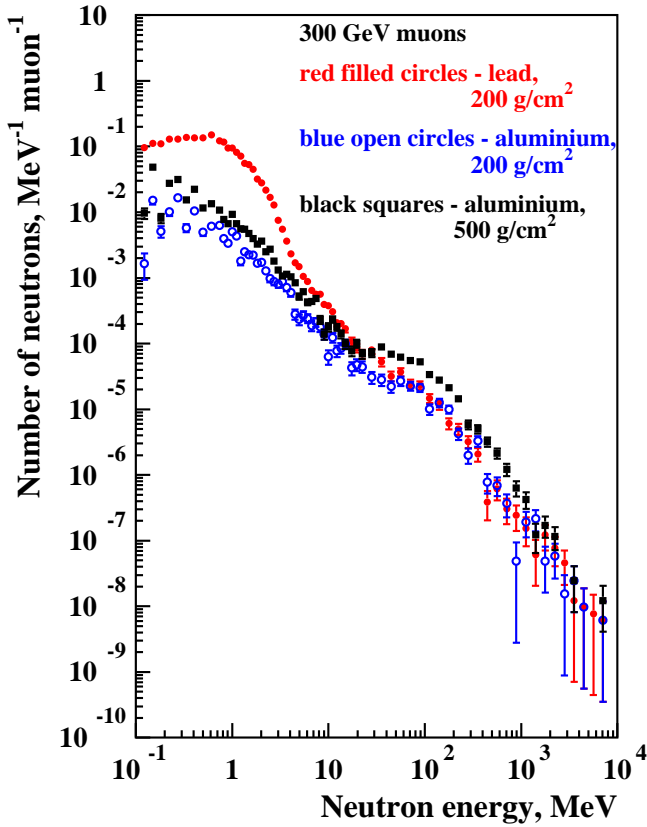


Fig. 7. Neutron energy spectra from 300 GeV muons in lead (thickness of 200 g/cm^2 – filled circles) and aluminium (thickness of 200 g/cm^2 – open circles and of 500 g/cm^2 – filled squares) as calculated with FLUKA (version of 2003).

with thickness of 200 g/cm^2 and 500 g/cm^2 . The spectra were obtained in the same way as above.

The figure demonstrates that the neutron flux increases with the increase of lead thickness from 200 g/cm^2 to 500 g/cm^2 but the enhancement is more pronounced at energies below 1-2 MeV. This is probably due to the secondary low-energy neutron production by higher energy neutrons. The neutron flux also increases with muon energy. The change in the neutron spectrum with muon energy is higher at neutron energies below a few MeV.

5 Background suppression strategies

A number of tools (both hardware and software) is available to suppress or tag neutron-induced background in underground physics experiments. To reduce background due to neutrons produced by natural radioactivity in the rock around the laboratory and in the detector materials, three ways have to be considered:

- A passive neutron shielding (made of water, polyethylene or other hydrogenous material) to suppress the external neutron flux due to the rock radioactivity, which is of the order of a few 10^{-6} neutrons/($\text{cm}^2 \text{ s}$). It

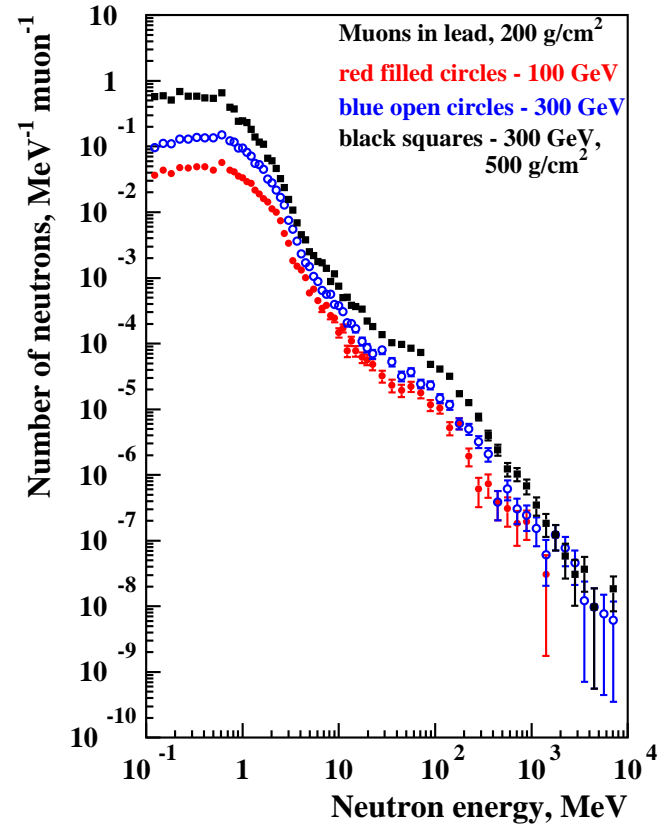


Fig. 8. Neutron energy spectra in lead from 100 GeV muons (thickness of 200 g/cm^2 – filled circles) and 300 GeV muons (thickness of 200 g/cm^2 – open circles; 500 g/cm^2 – filled squares) as calculated with FLUKA (version of 2003).

has been shown [7,8] that $50\text{-}60 \text{ g/cm}^2$ of polyethylene (possibly with lead) can reduce the neutron flux from the rock by six orders of magnitude.

- Special attention has to be paid to material selection for radiopurity. Neutron background in the detector (in the presence of a thick passive shielding, as indicated above) is mainly originated in the materials used in detector or shielding construction. This may eventually become the limiting background source.
- An active veto system can be installed just around the detector to tag neutrons produced in detector components [30,31]. A neutron can give a signal in - say - a dark matter detector, be scattered, slowed down and detected through its capture in the active veto system. Simultaneous detection of neutrons and/or γ -rays by the main target and veto can also be used to tag the background in $\beta\beta$ decay experiments.

Similarly, several methods have been proposed for the suppression or tagging of high-energy neutrons produced by muon interactions in the rock surrounding the detector and in the detector materials themselves, especially in the high- A γ -ray shielding.

- It is necessary to have an internal low- A neutron shielding, in order to shield the sensitive detector from neu-

trons produced by muon interactions in the rock and in the γ -ray shielding. A two- or three-layer shielding (external low- A (optional) + high- A + low- A) could be hence optimal for most applications.

- Since in muon-induced showers neutrons are accompanied by a large number of other secondaries, rejection tools based on veto or self-veto are extremely efficient. There is a large probability that a neutron is detected simultaneously with the primary muon or with other secondaries in the detector itself (self-veto) or in an active veto system [7, 25]. It was shown [7, 25] that in a large (250 kg) xenon-based dark matter detector, less than 5% of events with nuclear recoils are actually single nuclear recoils in the energy range of interest for dark matter searches. The remaining events contain energy deposition from nuclear recoils and muons or other secondaries produced by muons and hence do not mimic WIMP interactions. Similar result is expected for other detectors.
- The detector design has to be optimized, especially concerning the mass and position of high- A materials, since they may behave as neutron sources under muon irradiation.

Muon-induced neutron background depends strongly on the design of the experiment [32]. In particular, properties and placement of the materials close to the detector are extremely important, because they affect the muon showering and the propagation of secondaries. The shielding design has to be optimized as a compromise between the suppression of external radiation, the reduction of muon-induced background produced within the setup and the overall cost of the setup. Detector-specific and site-specific accurate Monte Carlo simulations are indeed required to achieve this goal.

Monte Carlo studies demonstrate that, with the choice of a suitable shielding and taking advantage from the tagging and rejection tools listed above, neutron-induced background does not represent a limitation for the existing and next-generation underground experiments at the depth of 2.5-4 km w. e., namely the depth of the European laboratories involved in ILIAS. In particular, the neutron background rate can be reduced down to a few events/tonne/year for direct dark matter experiments (corresponding to a potential cross-section sensitivity of 10^{-10} pb to spin-independent WIMP-nucleon interactions) [25] and to 10^{-3} events/(keV kg year) for neutrinoless $\beta\beta$ decay experiments [32].

6 Conclusions

Neutrons produced in underground laboratories either by natural radioactivity or by muons are an important background source for underground experiments looking for rare events (dark matter, neutrinoless $\beta\beta$ decay, low-energy neutrinos, etc.). Monte Carlo simulations play a crucial role for the estimate of the residual neutron-induced background and for the optimization of the rejection strategies.

It is necessary that simulations are as detailed as possible, including detector-related effects (like geometry and response).

The neutron flux due to radioactivity can be reliably predicted, using the combination of computer codes, such as SOURCES 4A for the estimate of the neutron yield and GEANT4/MCNPX for the description of neutron propagation and detection. The main systematic uncertainties are typically related to the knowledge of the chemical composition (and homogeneity) of the target material, and possibly to the (α, n) cross-sections. From the comparison between simulated neutron fluxes and measurements in underground laboratories (sect. 3.3), we can estimate the above uncertainty as about a factor of two. Since neutron flux from the laboratory rocks can be effectively shielded, neutrons emitted by detector components represent the main contribution to the total background, which may eventually limit the sensitivity. This background can be minimized by means of a careful material selection for radiopurity.

Neutron background induced by muon interactions is strongly dependent on the depth of the laboratory and on the experimental design, especially concerning position of high- A materials. In most cases neutrons produced by muon interactions in lead γ -ray shielding have to be suppressed by means of an internal neutron shielding made of hydrogenous materials. Since muon-induced showers contain a large number of particles, neutrons in the detector are often accompanied by other secondaries. For this reason, rejection methods based on simultaneous interactions of other particles in the detector itself (self-veto) or in an external veto are extremely efficient. To estimate reliably this effect, all particles produced in the showers have to be created and propagated in the Monte Carlo simulation. The two most-commonly used codes to describe the propagation of muon-initiated showers (GEANT4 and FLUKA) agree within a factor of two for the integral neutron yield. They both agree with measurements performed for low- A target materials (*e.g.* liquid scintillators), while seems to under-produce neutrons for heavier materials, such as lead (although experimental data are controversial and sometimes inconsistent). New experimental data are being collected in underground laboratories, that have to be considered together with a detailed Monte Carlo simulation accounting for detector-related effects.

Given the available suppression tools, neutron-induced background does not limit the sensitivity of existing and next-generation underground experiments at the depth of the ILIAS European laboratories, *i.e.* between 2.5 and 4 km w. e.

7 Acknowledgments

This work has been supported by the ILIAS integrating activity (Contract No. RII3-CT-2004-506222) as part of the EU FP6 programme in Astroparticle Physics (including the Ph.D. research of V. Tomasello). We would like to thank all our colleagues involved in the ILIAS activities, especially concerning Monte Carlo simulations (N3

and JRA1), in particular Drs. M. Robinson, R. Lemrani, M. J. Carson, H. Araújo and Mr. H. Chagani. We are grateful to the organizers of the ILIAS meeting at Chambéry for giving us an opportunity to present this review.

We dedicate this work to the memory of our friend and colleague Nicola Ferrari, who prematurely passed away in July 2006.

References

1. ILIAS, <http://ilias.in2p3.fr>.
2. GEANT4 Collaboration, S. Agostinelli *et al.*, Nucl. Instrum. and Methods A **506**, (2003) 250.
3. GEANT4 Collaboration, J. Allison *et al.*, IEEE Trans. Nucl. Sci. **53**, (2006) 270.
4. MCNPX, website <http://mcnpx.lanl.gov>.
5. A. Fassò *et al.*, *FLUKA: a multi-particle transport code*, CERN-2005-10 (2005), INFN/TC-05/11, SLAC-R-773; A. Fassò *et al.*, Computing in High Energy and Nuclear Physics 2003 Conference (CHEP2003), La Jolla, CA, USA, March 24-28, 2003, (paper MOMT005) eConf C0303241, hep-ph/0306267.
6. W.B. Wilson *et al.*, *Souces4A*, Technical Report LA-13639-MS, Los Alamos (1999).
7. M.J. Carson *et al.*, Astropart. Phys. **21**, (2004) 667.
8. R. Lemrani *et al.*, Nucl. Instrum. and Methods A **560**, (2006) 454.
9. V. Tomasello *et al.*, in preparation.
10. *Empire 2.19*, website <http://www.nndc.bnl.gov/empire219/>.
11. E. Tziaferi *et al.*, Astropart. Phys. **27**, (2007) 326.
12. B.E. Watt, Phys. Rev. **87**, (1952) 1037.
13. V. Chazal *et al.*, Astropart. Phys. **9**, (1998) 163.
14. F. Arneodo *et al.*, Nuovo Cimento A **112**, (1999) 819.
15. S. Fiorucci *et al.*, Astropart. Phys. **28**, (2007) 143.
16. R. Lemrani and G. Gerbier, J. Phys.: Conf. Ser. **39**, (2006) 145.
17. M. Aglietta *et al.*, Phys. Rev. D **58**, (1998) 092005.
18. M. Aglietta *et al.*, Phys. Rev. D **60**, (1999) 112001.
19. M. Aglietta *et al.*, Phys. Atom. Nucl. **66**, (2003) 123.
20. W. Rhode, Ph.D. Thesis, University of Wuppertal, WUB-DIS 93-11, 1993.
21. Ch. Berger *et al.*, Phys. Rev. D **40**, (1989) 2163.
22. P. Antonioli *et al.*, Astropart. Phys. **7**, (1997) 357.
V.A. Kudryavtsev *et al.*, Phys. Lett. B **471**, (1999) 251.
23. V.A. Kudryavtsev *et al.*, Nucl. Instrum. and Methods A **505**, (2003) 688.
24. Y.F. Wang *et al.*, Phys. Rev. D **64**, (2001) 013012.
25. H.M. Araujo *et al.*, Nucl. Instrum. and Methods A **545**, (2005) 398.
26. V. Chazal *et al.*, Nucl. Instrum. and Methods A **490**, (2002) 334.
27. L. Bergamasco *et al.*, Nuovo Cimento A **13**, (1973) 403.
28. G.V. Gorshkov *et al.*, Sov. J. Nucl. Phys. **18**, (1974) 57.
29. V.A. Kudryavtsev, Talk at the TAUP2007 Workshop; accessible from <http://www.awa.tohoku.ac.jp/taup2007/slides>.
30. M.J. Carson *et al.*, Nucl. Instrum. and Methods A **548**, (2005) 418.
31. C. Bungau *et al.*, Astropart. Phys. **23**, (2005) 97.
32. L. Pandola *et al.*, Nucl. Instrum. and Methods A **570**, (2007) 149.